

J-2-1

Evaluation of Chemical Structures and Work Function of NiSi near the Interface between Nickel Silicide and SiO₂

A. Ohta¹, H. Yoshinaga¹, H. Murakami¹, D. Azuma¹, Y. Munetaka¹,
S. Higashi¹, S. Miyazaki¹, T. Aoyama², K. Kosaka² and K. Shibahara^{1,3}

¹Grad. School of AdSM, Hiroshima Univ., Kagamiyama 1-3-1, Higashi-Hiroshima 739-8530, Japan

Phone: +81-824-24-7648, FAX: +81-824-22-7038, E-mail: semicon@hiroshima-u.ac.jp

²Fujitsu Laboratories Ltd., ³Research Center for Nanodevices and Systems, Hiroshima Univ.

1. Introduction

In the continuous CMOS scaling, the use of conventional poly-Si gate has been faced practically with serious limitations being related to a gate potential drop caused by the gate leakage current flowing through gate resistance and a depletion effect. To overcome such limitations, the implementation of alternative gate material with a lower resistivity is strongly needed. Ni-silicide is one of the most promising materials for metal gate because its work function value can be changed by chemical composition and impurity incorporation [1-5]. However, quantitative understanding on the mechanism to define effective work function of Ni-silicide has not been confirmed yet although the changes in electric dipoles at the interface with chemical composition, crystallographic orientation and impurities segregation are thought to be responsible for the work function variation.

In this work, pure and impurity-implanted Ni-silicides formed on SiO₂ were characterized by X-ray photoelectron spectroscopy (XPS), where the Ni-silicide/SiO₂ interfaces were analyzed through SiO₂ for the samples after removing the Si substrate from the backside in addition to the analysis from the surface side to evaluate the correlation between the effective work function and chemical composition or impurity concentration at the interface.

2. Experimental

After standard wet-cleaning steps of Si(100) wafer, poly-Si (~100nm) layer was deposited on thermally-grown SiO₂ (~7nm) followed by ion implantation of B⁺, P⁺, As⁺ and Sb⁺ with a dose of 1x10¹⁶ ions/cm² and activation annealing at 1000°C. The pure sample was also prepared with skipping ion implantation as a reference. Subsequently, Ni films in the thickness range from 70 to 80nm was formed on poly-Si and 2 step silicidation annealing was performed at 400 and 500°C. In some samples, the Si(100) substrates were completely removed by wet-etching. The backside etching was performed by the following process steps. Firstly, quartz substrate was attached on the Ni-silicides surface by a adhesive to support the etched sample. Next, the Si substrate was etched repeatedly using an HF+HNO₃+CH₃COOH solution diluted with ethanol until remaining Si thickness became below ~10µm. For further thinning of the Si substrate, Si selective etching was carried out using a warmed KOH solution with monitoring the thickness by Raman scattering and optical transmittance measurements. Residual K atoms on the sample surface were removed completely by pure water rinse.

3. Results and Discussion

Chemical bonding features at the Ni-silicide/SiO₂ interface were compared with those at the Ni-silicide surface as shown in Fig.1. For the pure Ni-silicide sample

prepared without implantation, Ni2p 3/2 signals originated from Ni-Si bonding units were clearly observed at a binding energy of ~853eV and almost no oxide component of Ni was observable both at the Ni-silicide surface and at the Ni-silicide/SiO₂ interface. The formation of Si-O bonds at the surface and at the interface was confirmed from Si2p spectra. Chemically-shifted Si2p signals due to Si-O bonding units were broadened toward the lower binding energy side even for the Si2p spectrum measured through the SiO₂ layer after the back side etching, in comparison to the reference spectrum of 2nm-thick thermally-grown SiO₂ on Si(100). This result indicates that the interface between NiSi and SiO₂ is not atomically flat. Notice that the average chemical composition Ni/(Ni+Si) at the interface was Si-rich as compared with that at the Ni-silicide surface. Similar results are obtained for implanted samples except the B-implanted case where both at the surface and at the interface were Si-rich. The chemical bonding features of implanted impurities such as Sb, B and P near the Ni-silicide/SiO₂ interface were investigated in comparison to those near the Ni-silicide surface as shown in Fig.2. For all cases, impurities bonded with Ni and/or Si atoms are dominant. No incorporation of implanted Sb and P into the thermally-grown SiO₂ layer and native surface oxide was observable but in contrast distinct pile-ups of Sb and P atoms near the Ni-silicide/SiO₂ interface were detected. On the other hand, for the B-implanted case, chemically-shifted B1s signals presumably due to suboxides were slightly observed at the Ni-silicide/SiO₂ interface and no pile-up of B atoms at the interface was measured. The chemical compositions of the samples are summarized in Table I.

To evaluate the effective work function at the Ni-silicide surface and at the interface for each sample, the threshold energy for photoelectrons was measured near the lower limit in the kinetic energy by fitting Fowler function [6]. In this work, to detect sufficient photoelectrons emitting with a low kinetic energy, negative bias as low as -15V was

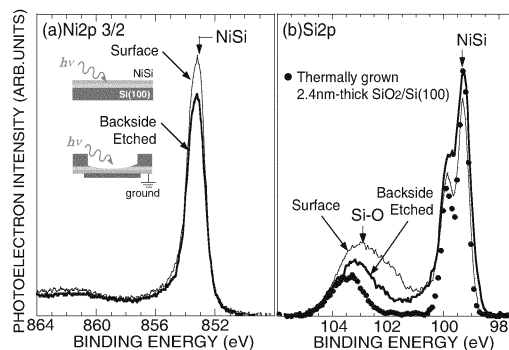


Fig.1. Ni2p3/2 (a) and Si2p (b) spectra for pure Ni-silicide, which were taken from the Ni-silicide surface and the near-interfacial region of Ni-silicide through the SiO₂ layer.

applied to the sample. For the calibration of this technique and setting a proper sample bias, we firstly measured the work functions of Au after removing surface carbon contaminants by Ar⁺ ion sputtering and confirmed that the measured values was the same as the reported ones within an accuracy with $\pm 0.05\text{eV}$ (Fig.3). In Fig. 3 the yield spectra near lower limit in the kinetic energy scale for the pure Ni-silicide sample, which were taken at the surface through the native oxide and at the interface through the thermally-grown SiO₂ layer, are compared. The potential drop in the oxide layer during the photoemission measurements, the kinetic energy scale was calibrated with O1s and Ni2p 3/2 core-line peaks. By fitting a Fowler function to measured spectra, the work function of pure Ni-silicide surface (4.74eV) was determined to be $\sim 0.2\text{eV}$ lower than that of Ni-silicide/SiO₂ interface (4.53eV).

The work functions of the samples evaluated by the above mentioned XPS measurement are plotted as functions of the Ni composition (Fig.4). The reported values of work function of Ni-silicide on SiO₂ or HfSiOx(N) are also plotted as references[2-5]. Similar values in the work function were obtained for the surfaces of the pure Ni-silicide, P-, Sb- and As-implanted cases. And we found that the effective work function at the interface of the Sb-implanted case is likely to be an extension of the change in the work function with the Ni composition seen in the surface and the interface of the pure Ni-silicide case, being similar to a trend reported on HfSiOx(N). For the Sb-implanted case, a decrease of Ni composition and the Sb pile-up seem to be responsible for a significant reduction of work function near the interface. Since the P pile-up at the Ni-silicide/SiO₂ interface is smaller by a factor of ~ 5 than the Sb pile-up, and the reduction of the work function for the P-implanted case is

thought to be mainly due to the reduction of Ni composition. In contrast, for the B-implanted case, although the average Ni content is about a half value of the pure Ni-silicide surface, the work function is not very different from the surface work function of the pure Ni-silicide and there is no significant difference between at the surface and at the interface. Considering that there is no distinct change in B incorporation between the interface and the surface, B incorporation is likely to reduce the work function as suggested from the reduction of density of states in valence band spectrum for the B-implanted sample.

In conclusion, for P-, Sb-implanted Ni-silicides, Ni composition rather than P and Sb pile-up is a major factor to change the work function, while for B-implanted Ni-silicide, B incorporation suppress a reduction in the work function with a decrease in Ni composition.

Acknowledgements

This work was supported in part by the STARC and the 21st Century COE program "Nanoelectronics for Terra-Bit Information Processing" in Hiroshima University from Ministry of Education, Science, Sports and Culture of Japan

References

- [1] J. Kedzierski et al., IEDM 2003. Tech. Dig. p.315.
- [2] J. A. Kittl et al., IEEE Electron Device Letters, 27 (2006)p.34.
- [3] K. Takahashi et al., IEEE Trans. Electron Devices, 51 (2004) p.91.
- [4] M. Niwa et al., Ext. Abst. 11th Workshop on Gate Stacks. (2006) p.7.
- [5] T. Nabatame et al., Ext. Abst. 11th Workshop on Gate Stacks.(2006) p.133.
- [6] "Statistical Mechanics: The Theory of the Properties of Matter in Equilibrium,"2nd ed. (Cambridge, England: University Press, 1966).

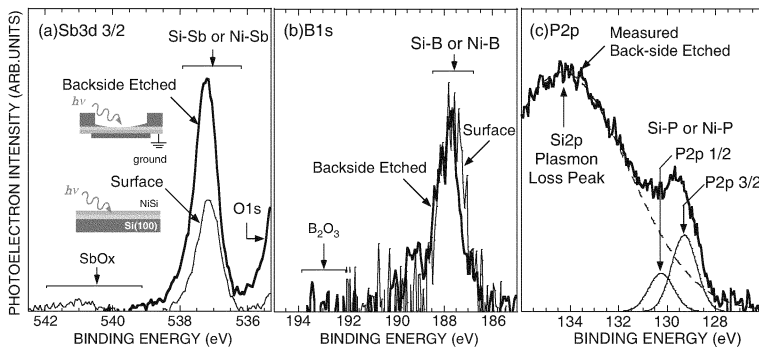


Fig.2. Sb3d3/2 (a), B1s (b) and P2p (c) spectra for Sb, B or P-implanted Ni-silicides, which were taken from their Ni-silicide surfaces and the Ni-silicide/SiO₂ interfaces.

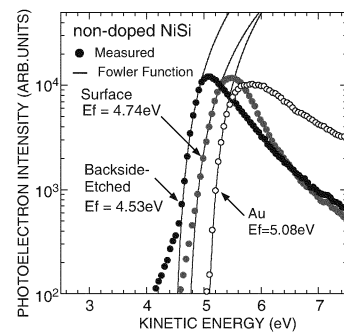


Fig.3. The yield spectra near the Fermi edge for the surface and at the interface of the pure Ni-silicide sample. The yield spectra for the Au after removing surface carbon contaminants by Ar⁺ ion sputtering were also shown as references. In addition, the curve fittings to the measured spectra with the use of a Fowler function are demonstrated.

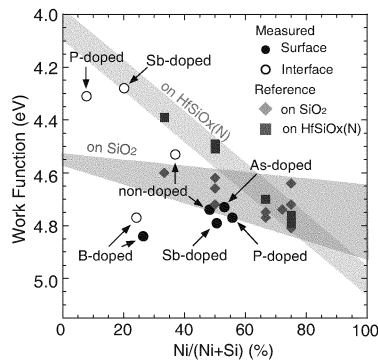


Fig.4. The effective work functions of the surfaces and the interfaces of Ni-silicides prepared with and without impurity implantation, which were determined by XPS measurements.

Table 1. Average chemical compositions of the Ni-silicide samples prepared with and without impurity implantation, which were measured near the surface and near the interface.

Sample	Chemical Composition (at.%)						Ni/(Ni+Si) (%)
	Si	Ni	Sb	B	P	As	
non	surface	51.8	48.2	—	—	—	48.2
	interface	63.0	37.0	—	—	—	37.0
Sb	surface	48.8	49.8	1.4	—	—	50.5
	interface	71.1	18.0	10.9	—	—	20.2
B	surface	67.5	24.1	—	8.4	—	26.3
	interface	71.2	22.8	—	6.0	—	24.3
P	surface	44.3	55.7	—	—	0.0	55.7
	interface	90.3	7.8	—	—	1.9	7.8
As	surface	43.0	57.0	—	—	0.0	57.0